SYNCHRONIZATION BETWEEN COUPLED OSCILLATORS: AN EXPERIMENTAL APPROACH

David Rijlaarsdam
Dept. of Mechanical Engineering
Eindhoven University of Technology
The Netherlands
D.J.Rijlaarsdam@student.tue.nl

Alexander Yu. Pogromsky
Dept. of Mechanical Engineering
Eindhoven University of Technology
The Netherlands
A.Pogromski@tue.nl

Henk Nijmeijer
Dept. of Mechanical Engineering
Eindhoven University of Technology
The Netherlands
H.Nijmeijer@tue.nl

Abstract

We present an experimental set-up that allows to study both controlled and uncontrolled synchronization between a variety of different oscillators. Two experiments are presented where uncontrolled synchronization between two types of identical oscillators is investigated. First, uncontrolled synchronization between two Duffing oscillators is investigated and second, uncontrolled synchronization between two coupled rotating elements is discussed. In addition to experimental results we provide both analytical and numerical results that support the experimental results.

Key words

Synchronization, Experiment, Duffing oscillator, Huygens experiments

1 Introduction

In the 17th century the Dutch scientist Christiaan Huygens observed a peculiar phenomenon when two pendula clocks, mounted on a common frame, seemed to 'sympathize' as he described it. What he observed was that both clocks adjusted their rhythm towards antiphase synchronized motion. This effect is now known as frequency or Huygens synchronization and is caused by weak interaction between the clocks due to small displacements of the connecting frame. In (Bennett *et al.*, 2002; Pantaleone, 2002; Senator, 2006; Kuznetsov *et al.*, 2007) an extended analysis of this phenomenon is presented. In (Oud *et al.*, 2006) the authors present an experimental study of Huygens synchronization and finally, in (Pogromsky *et al.*, 2003; Pogromsky *et al.*, 2006) a study of the uncontrolled as well as the controlled Huygens experiment is presented.

In this paper we present an experimental set-up (Tillaart, 2006) that allows to study both controlled and uncontrolled synchronization between a variety of different oscillators. In section 2 the set-up is introduced and we present the dynamical properties of the system. Furthermore, we present the means by which we are able to modify these properties to represent a variety of different oscillators. Next, in section 4, we present an experiment of the synchronization of two Duffing oscillators. We analyze the stability of the synchronization manifold and continue with numerical and experimental results. Section 5 presents an experiment where the set-up is adjusted to model two rotating eccentric discs which are coupled through a third disc mounted on a common axis. Conclusions and future research are presented in section 6.

2 Experimental Set-up

In order to experimentally study synchronization between coupled oscillators a set-up consisting of two oscillators, mounted on a common frame has been developed (see figure 1 and 2). The parameters of primary interest are presented in table 1. The set-up contains tree actuators and position sensors on all degrees of freedom. Furthermore, although the masses of the

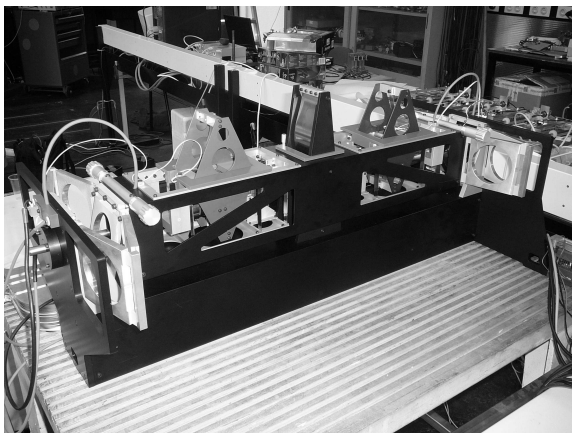

Figure 1. Photograph of the set-up.

oscillators (m) are fixed, the mass of the connecting beam (M) may be varied by a factor 10. This allows for mechanical adjustment of the coupling strength.

Table 1. Parameters in experimental set-up.

	Oscillator 1	Oscillator 2	Frame / beam
Mass	m	m	M
Stiffness	$\kappa_1(\cdot)$	$\kappa_2(\cdot)$	$\kappa_3(\cdot)$
Damping	$\beta_1(\cdot)$	$\beta_2(\cdot)$	$\beta_3(\cdot)$

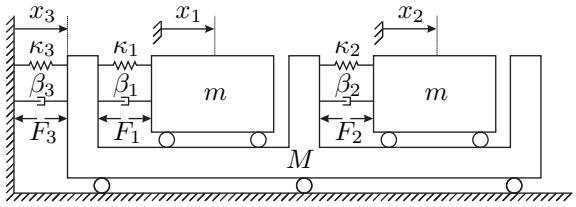

Figure 2. Schematic representation of the set-up.

A schematic representation of the set-up is depicted in figure 2 and the equations of motion are:

$$m\ddot{x}_1 = -\kappa_1(x_1 - x_3) - \beta_1(\dot{x}_1 - \dot{x}_3) + F_1 \quad (2.1)$$

$$m\ddot{x}_2 = -\kappa_2(x_2 - x_3) - \beta_2(\dot{x}_2 - \dot{x}_3) + F_2 \quad (2.2)$$

$$\begin{aligned} M\ddot{x}_3 &= \kappa_1(x_1 - x_3) + \kappa_2(x_2 - x_3) \quad (2.3)\\ &- \kappa_3\,(x_3) + \beta_1(\dot{x}_1 - \dot{x}_3) + \beta_2(\dot{x}_2 - \dot{x}_3) - \beta_3(\dot{x}_3)\\ &+ F_{\,3} - F_1 - F_2, \end{aligned}$$

where $m, M \in \mathbb{R}_{>0}$ and $x_i \in D_i \subset \mathbb{R},\ i = 1, 2, 3$ are the masses and displacements of the oscillators and the beam respectively. Functions $\kappa_i : \mathbb{R} \mapsto \mathbb{R},\ \beta_i : \mathbb{R} \mapsto \mathbb{R}$ describe the stiffness and damping characteristics present in the system. F_i are the actuator forces that may be determined such that the experimental set-up models a large variety of different dynamical systems (see 2.1).

The stiffness and damping in the system are found to be very well approximated by:

$$\kappa_i(q_i) = \sum_{j=1}^{5} k_{ij} q^j \quad (2.4)$$

$$\beta_i(\dot{q}_i) = b_i \dot{q}_i, \quad (2.5)$$

where $q_1 = x_1 - x_3$, $q_2 = x_2 - x_3$ and $q_3 = x_3$. The values of k_{ij} and $b_i\ \forall\ i = 1, 2, 3$ have been experimentally obtained and will be used to modify the systems' properties in the sequel.

2.1 Adjustment of the Systems' Properties

In order to experiment with different types of oscillators, the derived properties (stiffness and damping) are adjusted. Note that, since we know the damping and stiffness present in the system and we can fully measure the state of the system, we may adjust these properties, using actuators, to represent any dynamics we want. This allows modeling of different types of springs (linear, cubic), gravity (pendula) and any other desired effect within the limits of the hardware. In the next part of this paper we present two examples of this type of modulation. The system is first adapted to analyze synchronization between Duffing oscillators and secondly to analyze the synchronizing dynamics of two coupled rotating eccentric discs under the influence of gravity.

3 Definition of Synchronization

Before continuing with the experimental and analytical results the notion of synchronization should be defined in more detail. Due to the large amount of phenomena that seems to be gathered under the term synchronization, it is often difficult to correctly define synchronization. In (Pikovsky *et al.*, 2001) the authors introduce the concept of synchronization as:

Synchronization is the adjustment of rhythms of oscillating objects due to their weak interaction.

Although the above concept provides an insightful idea of synchronization a more rigorous definition is provided in (Blekhman *et al.*, 1997):

Definition 3.1: (Asymptotic Synchronization).
Given k systems with state $x_i \in X_i$ and output $y_i \in Y_i,\ i = 1, \ldots, k$ and given ℓ functionals $g_j : \mathcal{Y}_1 \times \ldots \times \mathcal{Y}_k \times \mathrm{T} \mapsto \mathbb{R}^1$, where T is a set of common time instances for all k systems and $\mathcal{Y}_i$ are the sets of all functions from T into the outputs Y_i. Furthermore defining a shift operator σ_τ s.t. $(\sigma_\tau y)(t) = y(t+\tau)$, we call the solutions $x_1(\cdot), \ldots, x_k(\cdot)$ of systems $\Sigma_1, \ldots, \Sigma_k$ with initial conditions $x_1(0), \ldots, x_k(0)$ *asymptotically synchronized w.r.t the functionals* $g_1, \ldots, g_\ell$ if:

$$g_j(\sigma_{\tau_1} y_1(\cdot), \ldots, \sigma_{\tau_k} y_k(\cdot), t) \equiv 0 \qquad \forall\ j = 1, \ldots, \ell \quad (3.1)$$

is valid for $t \to \infty$ and some $\sigma_{\tau_i} \in \mathrm{T}$.

Definition 3.2: (Approximate Asymptotic Synchronization).
Using the notations introduced in definition 3.1, we call systems $\Sigma_1, \ldots, \Sigma_k$ *approximately asymptotically synchronized w.r.t. to the functionals* $g_1, \ldots, g_\ell$ if for some sufficiently small $\varepsilon > 0$:

$$|g_j(\sigma_{\tau_1} y_1(\cdot), \ldots, \sigma_{\tau_k} y_k(\cdot), t)| \leqslant \varepsilon \qquad \forall\ j = 1, 2, \ldots, \ell \quad (3.2)$$

is valid for $t \to \infty$ and some $\sigma_{\tau_i} \in \mathrm{T}$.

In the sequel definition 3.1 and 3.2 will be used to define (approximate) synchronization.

4 Example 1: Coupled Duffing Oscillators

In this section experimental results with respect to two synchronizing Duffing oscillators are presented. After introducing the dynamical system an analysis of the limiting behaviour of the system is presented. Finally, both numeric and experimental results are presented and discussed.

4.1 Problem Statement & Analysis

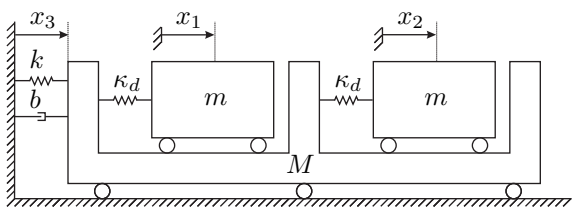

Figure 3. Schematic representation of the set-up modeling two coupled Duffing oscillators.

Consider the system as depicted in figure 3, where:,

$$\frac{\kappa_d(q_i)}{m} = \omega_0^2 q_i + \vartheta q_i^3 \tag{4.1}$$

where $q_i = x_i - x_3$ and constants $\omega_0,\ \vartheta \in \mathbb{R}_{>0}$.

The system under consideration represents two undriven, undamped Duffing oscillators coupled through a third common mass. The set-up depicted in figure 2 can be adjusted to model this system by defining the actuator forces as:

$$F_i = \kappa_i(q_i) + \beta_i(\dot{q}_i) - \kappa_d(q_i),\ i = 1, 2 \tag{4.2}$$
$$F_3 = 0 \tag{4.3}$$

Where $F_3 = 0$ is chosen because, in the original set-up, the beam already models the situation as depicted in figure 3 (linear stiffness and damping) fairly accurate. The equations of motion of the resulting system are:

$$m\ddot{x}_1 = -\kappa_d(x_1 - x_3) \tag{4.4}$$
$$m\ddot{x}_2 = -\kappa_d(x_2 - x_3) \tag{4.5}$$
$$M\ddot{x}_3 = \kappa_d(x_1 - x_3) + \kappa_d(x_2 - x_3) - kx_3 - b\dot{x}_3, \tag{4.6}$$

where $k, b \in \mathbb{R}_{>0}$ are the stiffness and damping coefficients of the beam.

Before continuing with the experimental and numerical results the systems' limiting behaviour is analyzed. In order to do so the notion of anti-phase synchronization needs to be defined:

Definition 4.1:((Approximate) Anti-phase Synchronization).
Consider two systems Σ_1 and Σ_2 with initial conditions x_{10} and x_{20} and corresponding solutions $x_1(x_{10}, t)$ and $x_2(x_{20}, t)$. Furthermore, assume that both $x_1(x_{10}, t)$ and $x_2(x_{20}, t)$ are periodic in time with period T. We call the solutions of $x_1(x_{10}, t)$ and $x_2(x_{20}, t)$ (approximately) asymptotically synchronized in *anti-phase* if they are (approximately) asymptotically synchronized according to definition 3.1 or 3.2, with:

$$g(\cdot) = x_1(\cdot) - \alpha\sigma_{\left(\frac{T}{2}\right)}x_2(\cdot), \tag{4.7}$$

with $\alpha \in \mathbb{R}_{>0}$ a scale factor and $\sigma_{\left(\frac{T}{2}\right)}$ a shift operator over half an oscillation period.

Using definition 4.1 it can been shown that the dynamics of the oscillators in (4.4) - (4.6) converges to anti-phase synchronization as $t \to \infty$ (see Lemma 4.1 below).

Lemma 4.1: (Global Asymptotic Stability of the Synchronization Manifold).
Consider the system of nonlinear differential equations (4.4) - (4.6). The trajectories of the oscillators Σ_1 and Σ_2 will converge to anti-phase synchronized dynamics, according to definition 4.1 as $t \to \infty$ for all initial conditions.

Proof (of Lemma 4.1).
Consider the system (4.4) - (4.6). To analyze the limit behaviour of this system, the total energy is proposed as a candidate Lyapunov function:

$$\mathcal{V} = \frac{1}{2}\sum_{i=1}^{3} m_i\dot{x}_i^2 + \sum_{i=1}^{3}\int_0^{\xi_i} \kappa_i(s)\, ds, \tag{4.8}$$

where $m_1 = m_2 = m$, $m_3 = M$, $\xi_i = x_i - x_3,\ i = 1, 2$, $\xi_3 = x_3$, $\kappa_i(q_i) = \kappa_d(q_i)$ and $\kappa_3 = kx_3$. Calculating the time derivative of $\mathcal{V}$ along the solutions of the system (4.4) - (4.6) yields:

$$\dot{\mathcal{V}} = -b\dot{x}_3^2. \tag{4.9}$$

Hence, we find $\dot{\mathcal{V}} \leq 0$ and the system may be analyzed using LaSalle's invariance principle.

Equation (4.9) implies that $\mathcal{V}$ is a bounded function of time. Moreover, $x_i(t)$ is a bounded function of time and will converge to a limit set where $\dot{\mathcal{V}} = 0$. On this limit set $\dot{x}_3 = \ddot{x}_3 = 0$, according to (4.9). Substituting this in system (4.4) - (4.6) yields $x_3 = 0$ on the

systems' limit set. Substituting $x_3 = \dot{x}_3 = \ddot{x}_3 = 0$ in (4.6) shows:

$$\kappa_d(x_1) = -\kappa_d(x_2) \tag{4.10}$$

Since κ_d is a one-to-one, odd function, this implies:

$$x_1 = -x_2 \tag{4.11}$$

Finally, substituting $x_1 = -x_2$ in (4.4) - (4.5) yields:

$$\dot{x}_2 = -\dot{x}_1. \tag{4.12}$$

Summarizing, it has been shown that any solution of (4.4) - (4.6) will converge to anti-phase synchronized motion according to definition 4.1 as $t \to \infty$. □

The next paragraph will present numerical and experimental results that support the analysis provided in this section.

4.2 Experimental & Numerical Results

In order to experimentally investigate the synchronizing behaviour of two coupled Duffing oscillators the set-up has been modified as specified in the previous paragraph. The oscillators are released from an initial displacement of -3 mm and -2.5 mm respectively (approximately in phase) and allowed to oscillate freely.

Figure 4 shows the sum of the positions of the oscillators and the position of the beam v.s. time. As becomes clear from figure 4, approximate anti-phase synchronization occurs within 40 s. Furthermore, figure 5 shows the limiting behaviour of both oscillators and the beam. Although the amplitudes of the oscillators differ significantly, the steady state phase difference is 1.01π. The most probable cause for the amplitude difference is the fact that the oscillators are not exactly identical. As a result, the beam does not come to a complete standstill, although it oscillates with an amplitude that is roughly ten times smaller than that of the oscillators.

In addition to the experimental results, numerical results are provided in figure 6 and 7. The parameters in the simulation are chosen as shown in table 2.

Table 2. Parameters in numerical simulation.

$\omega_o = 15.26$	$\vartheta = 8.14$	$M = 0.8$
$m = 1$	$k = 1$	$b = 5$

The results presented in figure 6 and 7 correspond to the experimental results provided in 4 and 5 respectively. Although the oscillation frequencies of the oscillators are almost equal (within 5%) in the simulation

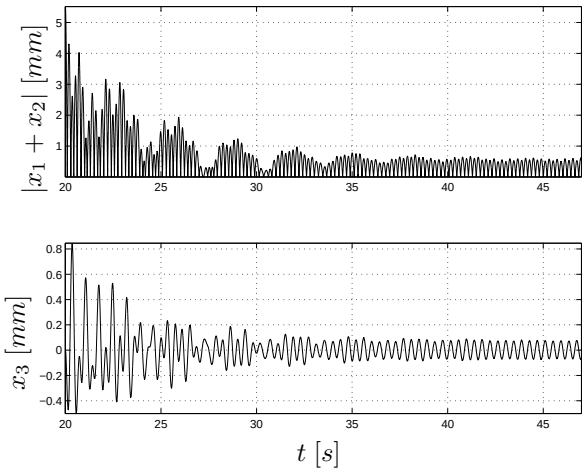

Figure 4. Experimental results: (top) Sum of the displacements of both oscillators. (bottom) Displacement of the connecting beam.

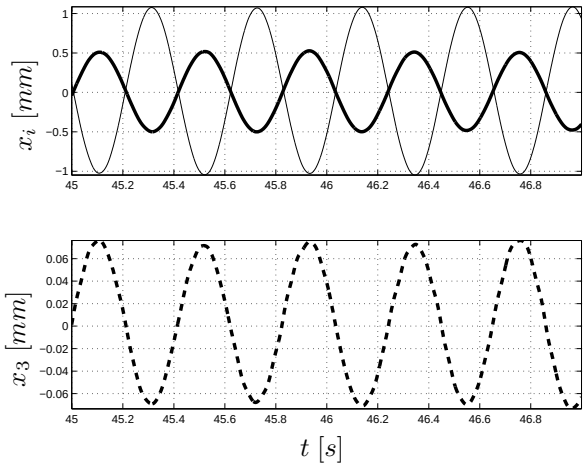

Figure 5. Experimental results: Steady state behaviour of the system. (top) Displacement of the oscillators (- x_1, - x_2). (bottom) Displacement of the connecting beam.

and the experiment, the final amplitudes of the oscillators differs by a factor 15. This is due to the fact that in the experiment the damping is over compensated, resulting in larger amplitudes of the oscillators. This presents no problem since the residual energy may dissipate through the motion of the beam, which does not come to a complete standstill due to the amplitude difference between the oscillators. In the numerical simulation almost exact anti-phase synchronization with equal oscillator amplitudes is achieved and this mechanism fails.

Finally, note that some of the differences between the experimental and simulation results may be coped with by tuning either the parameters of the numerical simulation or those of the set-up itself. *The question of identifying a model can thus be reversed to tuning the parameters of the set-up rather than those of the model.*

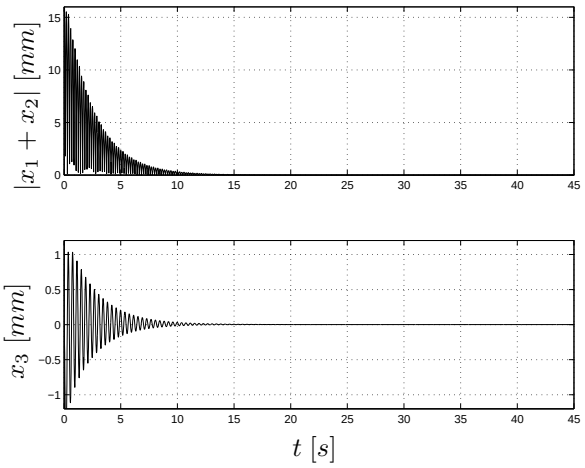

Figure 6. Numerical results: (top) Sum of the displacements of both oscillators. (bottom) Displacement of the connecting beam.

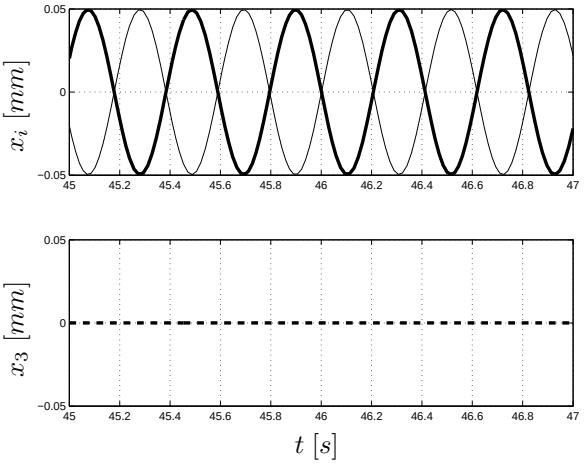

Figure 7. Numerical results: Steady state behaviour of the system. (top) Displacement of the oscillators (- x_1, - x_2). (bottom) Displacement of the connecting beam.

5 Example 2: Two Coupled Rotary Elements

Next to the synchronization of Duffing oscillators we investigated synchronization in a system of coupled rotating disc as depicted in figure 8. First the dynamics of the system will be specified in more detail and next experimental results will be presented.

5.1 Problem Statement

Consider the system as depicted in figure 8. This system consists of three discs. Discs 1, 2 represent the oscillators and disc 3 is connected to both other discs by torsion springs with stiffness k. Each of the discs has an eccentric mass at a distance ℓ_i from it's center ($\ell_1 = \ell_2 = \ell$). Furthermore the middle disc is coupled to the world by a torsion spring with stiffness k_3 and a torsion damper with constant b. The rotation of the discs is represented w.r.t. the world by the angles θ_i.

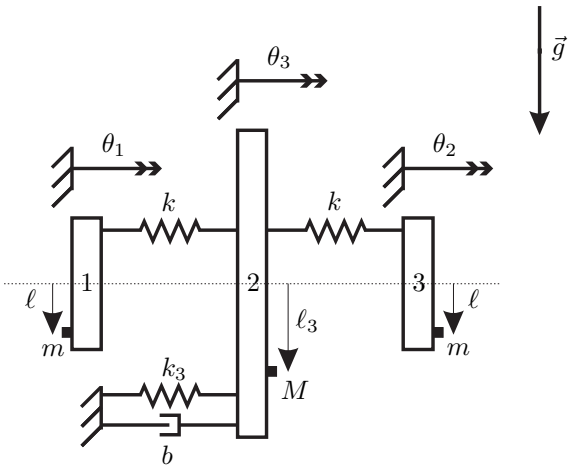

Figure 8. Schematic representation of the set-up modeling two coupled rotating elements.

The equations of motion of the system depicted in figure 8 are:

$$\ddot{\theta}_i = -\vartheta_i \left(k\left(\theta_i - \theta_3\right) + \delta_i \sin\theta_i\right),\ i = 1, 2 \quad (5.1)$$

$$\ddot{\theta}_3 = \vartheta_3\Big(\sum_{j=1}^{2} k\left(\theta_j - \theta_3\right) - k_3\theta_3 - b_3\dot{\theta}_3 - \delta_3 \sin\theta_3\Big), \quad (5.2)$$

with $\vartheta_i = \frac{1}{m\ell_i^2 + J_i}$ and $\delta_i = m_i g \ell_i$. The modification to the set-up is now more involved than in the previous example. First of all, the translation coordinates x_i should be mapped to rotation angles θ_i (arbitrary mapping). Secondly, in case of the Duffing oscillator the actuation forces F_1 and F_2 were meant to act on both the oscillators and the connecting mass. In the situation depicted in figure 8 the actuation force generated to model the coupling between the oscillator discs and the middle disc by means of the torsion spring should again act on the oscillators and the connecting beam in our set-up. However, the part of the actuation force that models the influence of gravity on the oscillators should only act on the oscillators and not on the connecting beam, since in figure 8 the gravity on discs 1 and 2 exerts a force only on the corresponding disc and not directly on the middle mass.

In order to adjust the set-up in figure 2 to model the system in figure 8 the actuator forces are defined as:

$$F_i = \kappa_i(q_i) + \beta_i(\dot{q}_i) - \vartheta_i\left(\eta_i + g_i\right), i = 1, 2 \quad (5.3)$$

$$F_3 = \kappa_3(x_3) - \vartheta_3\left(\eta_3 + g_3\right) - \tilde{g}(\cdot), \quad (5.4)$$

with $\kappa_i(q_i)$ and $\beta_i(\dot{q}_i)$ as defined earlier, $\eta_i = k\left(\theta_i - \theta_3\right),\ i = 1, 2$, $g_i = \delta_i \sin\theta_i$ and $\tilde{g} = \sum_{j=1}^{2} \vartheta_i g_i$. Damping is left to be the natural damping of the beam

in the set-up. Furthermore, translation is mapped to rotation angles according to: $\theta_i = \frac{\pi}{2}\frac{x_i}{x_i^\star}$, with $x_i^\star$ is the maximal displacement of the oscillators and the beam, assuring $\pm$ 90° turns in the rotation space.

5.2 Experimental Results

Experimental results, are presented in figure 9 and 10. It becomes clear that approximate anti-phase synchronization occurs after about 20 s. Again complete synchronization does not occur because the oscillators are not identical. In addition figure 10 shows the steady state behaviour of the rotating system, from which the approximate anti-phase synchronized behaviour becomes clear immediately.

6 Conclusion & Future Research

We presented a set-up capable of conducting synchronization experiments with a variety of different oscillators. Two sets of experimental results were provided that show the potential of this set-up. First we modeled and experimentally obtained synchronization between two coupled Duffing oscillators. Second, we showed that it is possible to model systems with rotating dynamics and to effectively model the local influence of gravity in this case.

In addition to studying uncontrolled synchronization the set-up has the potential to study controlled synchronization. Furthermore, we aim to model the Huygens set-up and perform controlled and uncontrolled synchronization experiments with this type of dynamical system.

7 Acknowledgements

This work was partially supported by the Dutch-Russian program on interdisciplinary mathematics '*Dynamics and Control of Hybrid Mechanical Systems*' (NWO grant 047.017.018).

References

Bennett, M., M. Schat, H. Rockwood and K. Wiesenfeld (2002). Huygens's clocks. *Proceedings of the Royal Society A: Mathematical, Physical and Engineering Sciences* **458**(2019), 563–579.

Blekhman, I.I., A.L. Fradkov, H. Nijmeijer and A.Yu. Pogromsky (1997). On self-synchronization and controlled synchronization. *System & Control Letters* (31), 299 – 305.

Kuznetsov, N.V., G.A. Leonov, H. Nijmeijer and A.Yu. Pogromsky (2007). Synchronization of two metronomes,. *3rd IFAC Workshop 'Periodic Control Systems'*. St. Petersburg, Russian Federation.

Oud, W., H. Nijmeijer and A.Yu. Pogromsky (2006). A study of huygens synchronization. experimental results. *Proceedings of the 1st IFAC Conference on Analysis and Control of Chaotic Systems, 2006*.

Pantaleone, J. (2002). Synchronization of metronomes. *American Jounal of Physics* **70**(10), 992–1000.

Pikovsky, A., M. Rosenblum and J. Kurths (2001). *Synchronization, A universal concept in nonlinear sciences*. Cambridge Nonlinear Science Series. Cambridge University Press.

Pogromsky, A.Yu, V.N. Belykh and H. Nijmeijer (2003). Controlled synchronization of pendula. *Proceedings 42rd IEEE Conference on Decision and Control* pp. 4381–4368.

Pogromsky, A.Yu, V.N. Belykh and H. Nijmeijer (2006). *Group Coordination and Cooperative Control*. Chap. A Study of Controlled Synchronization of Huygens' Pendula, pp. 205–216. Vol. 336 of *Lecture Notes in Control and Information Sciences*. Springer.

Senator, M. (2006). Synchronization of two coupled escapement-driven pendulum clocks. *Journal of Sound and Vibration* **291**(3-5), 566–603.

Tillaart, M.H.L.M. van den (2006). Design of a mechanical synchronizing system for research and demonstration purooses for d&c. Master's thesis. Eindhoven University of Technology.

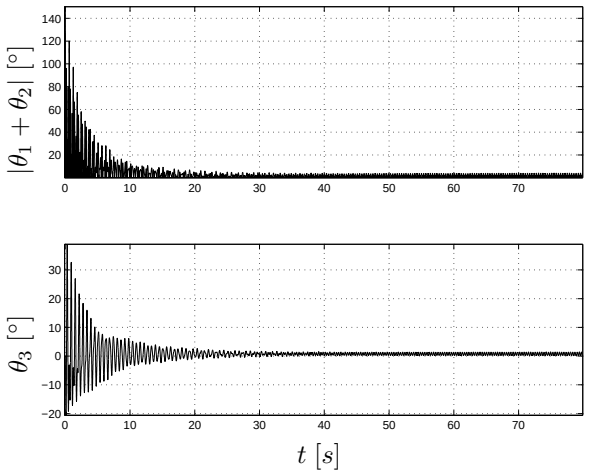

Figure 9. Experimental results: (top) Sum of the rotation angles of the outer discs. (bottom) Rotation angle of the connecting disc.

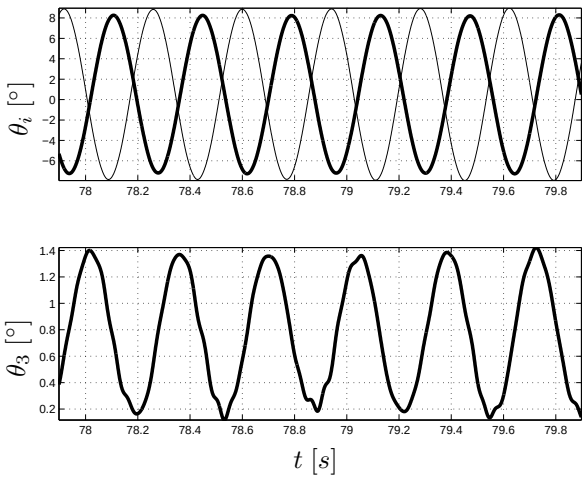

Figure 10. Experimental results: Steady state behaviour of the system. (top) Outer discs (- θ_1, - θ_2). (bottom) Connecting disc.